Metals Materials And Processes, 2000, Vol. 12, No. 2 & 3, pp. 127 - 142.

PRESSURE INDUCED PHASE TRANSITIONS IN NICKEL AND CHROMIUM BASED ALLOYS

T G Ramesh and V Shubha
Materials Science Division, National Aerospace Laboratories, Bangalore 560017, India

(Received 10 January 2000)

Abstract: This article describes the developments carried out in our laboratory in establishing absolute thermoelectric power (TEP) and AC resistivity as powerful diagnostic tools to study continuous phase transitions at high pressures. The teflon cell arrangement and the pyrophyllite-talc assembly for measurement of TEP and resistivity used in the conventional piston - cylinder high pressure apparatus will be discussed. A PC based data acquisition system designed for high-resolution measurement of these electronic transport properties of conducting solids at ambient and high pressures as a function of temperature will be described in some detail. The power of these techniques will be demonstrated through new observations on a pressure induced second order transition in nickel and in commensurate - paramagnetic and incommensurate-paramagnetic transitions in some chromium based alloys.

Keywords: Thermopower, high pressure, magnetic transition, nickel, chromium alloys.

1. INTRODUCTION

TEP is perhaps the most sensitive among the electronic transport properties in metallic systems. This stems from the well known Mott and Jones relation[1] connecting TEP with the energy derivative of the density of states and the relaxation time of the conduction electrons evaluated at the Fermi energy. In the field of high pressures, apart from the pioneering work of Bridgman[2], TEP has not been used extensively to study the electronic structure of materials. This is mainly due to experimental problems associated with the measurement of TEP at high pressures and high temperatures. In this direction we have developed several techniques[3-8] for measurement of this property under controlled conditions of temperature and pressure.

The conventional method of measuring the resistivity of a sample using the four probe technique as a function of temperature requires six leads to be brought out from the high pressure environment to ambient pressure conditions. In this context an AC resistivity set up using the lock-in technique suitable for high pressure studies has been developed[9] where only four probes are employed in a way similar to the arrangement employed for TEP measurement.

A PC based data acquisition system for high resolution measurement of TEP and AC resistivity, designed and fabricated in our laboratory[8], facilitates simultaneous measurement of both these properties under identical conditions of temperature and pressure.

Pressure studies on nickel have generated considerable controversy regarding the existence of a second order phase transition near 10 kbar[10]. In contrast to several recent investigations, we observe well defined anomalies in both resistivity and TEP near 10 kbar at ambient temperature which provide new and conclusive evidence for the existence of a pressure induced phase transition in nickel. A theoretical model based on polarity fluctuations between close lying $3d^8\ 4s^2$ and $3d^9\ 4s^1$ configurations has been developed to account for several anomalies in the physical properties of Ni near 10 kbar.

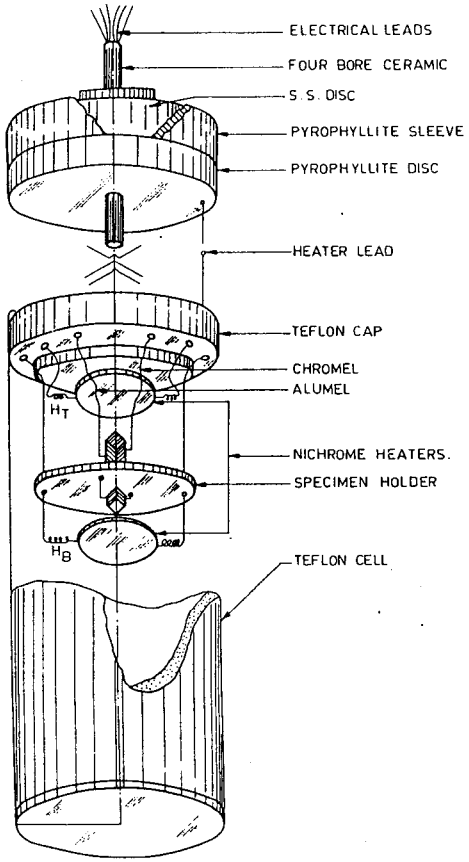

Fig. 1. Teflon cell assembly for TEP and Resistivity studies

Chromium a

riety of magnetic transitions and have been studied extensively at ambient pressure and also at high pressures[11-14]. Among the transport properties, only resistivity has been extensively used to track the magnetic phase boundaries in these alloy systems in the P-T plane. Extensive measurements carried out in this laboratory[15-17] where both resistivity and TEP are used as diagnostic tools to delineate magnetic phase boundaries clearly show that resistivity is a insensitive technique to track these phase boundaries especially in the high pressure region.

In this paper we review the development of TEP and AC resistivity techniques and the associated PC based instrumentation for high resolution measurement of these properties in the pressure range 0-50 kbar and up to 1000°C. The power of these techniques especially TEP is demonstrated through new observations on pressure induced second order transition in Ni and direct evidence for commensurate-incommensurate transition in chromium based alloys.

2. TEFLON CELL TECHNIQUE

In high pressure studies using the Piston-Cylinder apparatus, the teflon cell technique for generating pressures up to 50 kbar has been extensively used[18]. The main advantage of the teflon cell technique is that the use of a liquid (petroleum ether, silicone fluid, isomyl alcohol etc.,) as the pressure transmitting medium ensures a near hydrostatic environment for the sample under study. The use of an internal heating arrangement facilitates the measurement of the properties under study (TEP and AC resistivity) up to 300°C. Figure 1 shows the typical arrangement for TEP measurement on a metallic sample[3]. In order to create a steady temperature difference between the ends of the specimen, the teflon container has been partitioned as shown in the figure to minimize the convection mixing of the silicone oil which is used as a pressure transmitting medium. The silicone oil in the two compartments is heated to different temperatures using two nichrome heaters of different resistance values, which are connected in parallel. Chromel-Alumel thermocouple probes are spot welded to the sample at either ends and brought out from high pressure to the atmospheric pressure region in a way similar to that described in reference 18. This design of the thermopower cell allows one to maintain a constant temperature difference between the ends of the sample, which can be varied between 0.1°C to 10°C.

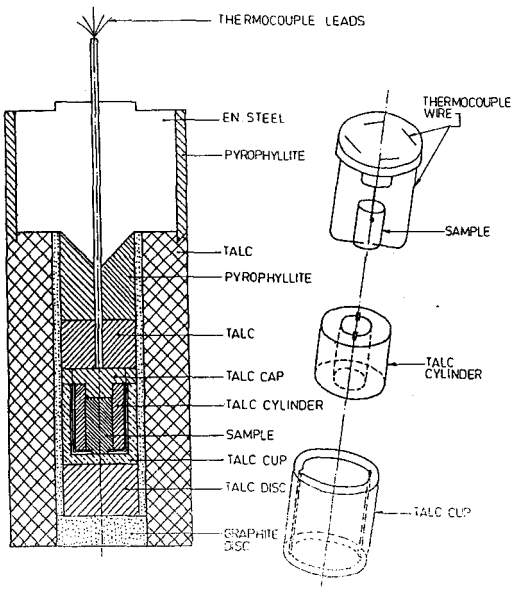

Fig. 2. High Temperature cell assembly for TEP and Resistivity studies

3. HIGH TEMPERATURE CELL

The design of the high temperature - high pressure thermopower cell[4] suitable for studies up to 1000°C is shown in Fig. 2. The specimen is generally in the form of a right cylinder of 5-mm diameter and 3 mm long. It is encased in a boron nitride (BN) sleeve with 1.5-mm thick walls. The four leads of the two thermocouple probes are embedded in to the specimen and are taken out through the holes in the sleeve along the grooves (90° apart) made on its surface. These four leads are brought out from the high pressure to the atmospheric pressure region in a way similar to that employed in the teflon cell technique.

The graphite sleeve shown in the figure serves as a heater for the cell assembly. The temperature profile in this tubular graphite furnace has a non-uniform temperature zone near the ends. Since the specimen has to be subjected to a temperature gradient for measurement of thermoelectric power, the natural temperature profile of the furnace was exploited by proper positioning of the sample in the assembly. The graphite heater is powered by a high current low voltage source.

4. PC BASED TEP MEASURING SYSTEM

The absolute Thermopower, S, of the sample, in the differential mode of measurement is given by the general expression[1]

$$S(T) = S_{Chr}(T) - S_{Chr-Alu}(T)\left[\frac{V_{Chr-Sam-Chr}}{V_{Chr-Sam-Chr} - V_{Alu-Sam-Alu}}\right]$$

Here S_{Chr} (T) and $S_{Chr-Alu}$ (T) are absolute TEP of chromel and the relative TEP of the chromel - alumel thermocouple respectively. $V_{Chr-Sam-Chr}$ and $V_{Alu-Sam-Alu}$ are the differential voltages developed across the thermocouple formed out of the reference probes and the specimen, when a small temperature difference is maintained between the ends of the sample. T is the mean temperature of the sample. It is clear from the above relation that in order to evaluate S as a function of mean temperature, it is necessary to simulate the temperature dependence of both S_{Chr} and $S_{Chr-Alu}$.

Figure 3 gives the block diagram of the PC based TEP measuring system[6,8] useful for either ambient or high pressure studies. The design of the system is centered on a precision temperature controller / programmer[7] developed for usage with both the teflon and the high temperature thermopower cell arrangement. It essentially comprises of the

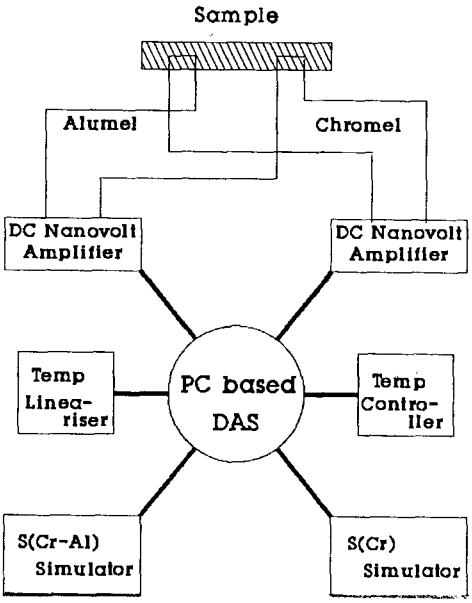

Fig. 3. Block diagram of the PC based TEP measuring system

following sub systems viz., signal amplifier with cold junction compensation, 16 bit A/D converter, a temperature linearising software, a software for simulation of the PID algorithm, a D/A converter and a Power amplifier. The power requirement for attaining temperatures up to 300°C in the teflon cell using nichrome heater is around 90 watts while it is around 1 kilo watt for the graphite heater assembly where temperature around 1000°C is attained. A significant aspect of this instrumentation is that a temperature stability of ± 0.02°C has been achieved in the teflon cell arrangement while it is around ± 0.05°C in the high temperature thermo- power cell. This is nearly two orders of magnitude superior to that quoted by others in the field of high pressures. It is obvious that a temperature controller with sufficiently fast control action can be easily converted to a temperature programmer. If the set point value in the PID algorithm is increased linearly with respect to time, the temperature of the sample would follow suit provided the heating rate selected is slower than the rate of control action. Linear rate of heating/cooling which is software selectable from 1°C to 10°C /minute makes this system useful for other techniques such as high pressure DTA and studies on non equilibrium systems like glasses.

An important requisite for TEP measurement is the control of temperature gradient. The control of the gradient should be such that, while the mean temperature is held constant, the magnitude of the temperature difference across the ends of the sample can be altered at will. Since TEP in the differential mode of measurement is related to the limiting value of $V_{Chr\text{-}Sam\text{-}Chr}$ / ($V_{Chr\text{-}Sam\text{-}Chr}$ - $V_{Alu\text{-}Sam\text{-}Alu}$) as the temperature difference tends to zero, the system should have the facility to evaluate this quantity for different temperature differences keeping T constant. These requirements have been achieved by employing two separate temperature controllers. The mean temperature T is one of the controlled variables while the temperature gradient can be varied independently by controlling the temperature of one of the ends of the sample by a separate controller.

The non-linear variations with temperature of the physical quantities like the absolute TEP of chromel (S_{Chr}) and the relative TEP of chromel-alumel thermocouple ($S_{Chr\text{-}Alu}$) are simulated by employing a sixth order polynomial curve fitting algorithm. This procedure forms the basis for the two simulators shown in the block diagram (Figure 3).

The differential thermoelectric voltages ($V_{Chr\text{-}Sam\text{-}Chr}$) and ($V_{Alu\text{-}Sam\text{-}Alu}$) are separately amplified using high stability low drift DC amplifiers (Keithley Nanovolt amplifiers, Model 181). After real time digital filtering, these output voltages are accessed in the PC through a data acquisition system (DAS). DAS employed for these studies is a Keithley model 575 system with a ten channel multiplexed 16bit A/D converter and a two channel 14 bit D/A converter. The absolute TEP of the sample can then be computed in real time using appropriate software to compute the relevant parameters in the expression for TEP.

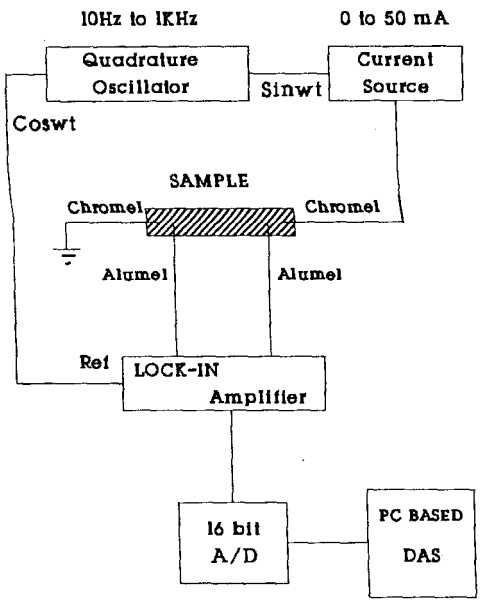

Fig. 4. Schematic of the AC Resistivity setup

In the isobaric mode where TEP is studied as a function of mean temperature, the ramp of the temperature programmer is utilized where the rate of heating, temperature increment at which the data has to be collected and the range of temperature to be covered are all software selectable. In the isothermal mode of measurement, the temperature of the sample is held constant to within $\pm$ 0.02°C and TEP data is collected as a function of pressure. The overall accuracy in TEP measurement in our system is 0.5% and the resolution is $\approx 0.01 \mu V/^{o}C$.

5. AC RESISTIVITY SETUP

The standard four-probe method of measuring resistivity as a function of temperature at high pressures generally requires six leads to be brought out of the high pressure cell of diameter less than 12 mm. This poses some experimental difficulties. We have developed a novel technique[9] for AC resistivity measurement where only four leads are taken out from the high pressure cell. The two pairs of thermocouples spot welded to the sample at either ends (same arrangement as in the TEP cell) are used for passing the AC current (across chromel-sample-chromel), measuring the AC voltage developed across the sample (alumel-sample-alumel), and also for measuring the temperature (DC voltage developed across the thermocouples).

Figure 4 gives the block diagram of the AC resistivity set up. The system consists of a quadrature oscillator, a high output impedance AC constant current source and a Lock-in-amplifier interfaced to a PC based DAS. The quadrature oscillator constructed out of two analog multipliers features two sine wave outputs at quadrature whose frequency can be varied from 10 Hz to 1 kHz. One of the sine wave outputs forms the reference signal for the Lock-in-Amplifier while the other output drives a constant current source. The design of the constant current source is centered on the well-known Howland circuit. It would suffice here to mention that the magnitude of the current could be varied continuously from 0 to 50 mA and the high output impedance ($\approx$ several megaohms) ensures that the current through the metallic sample is constant irrespective of its impedance. The AC voltage developed across the sample that is proportional to the sample resistance is measured with a DSP Lock-in-Amplifier (Stanford Research Systems, Model SR 830) configured for selective external mode of operation. This ensures high sensitivity and full phase control. The frequency of the AC signal is chosen to be 400 Hz to minimize the line frequency noise. The output voltage from the Lock-in-amplifier is accessed directly to the PC through its IEEE 488 interface.

Simultaneous measurement of temperature is achieved by measuring the DC component of the differential voltage developed across the current and the voltage leads which are in close proximity. The contribution to the DC voltage from the small portion of the sample between these two leads is negligible if one invokes the Law of Intermediate metals. A low pass active filter essentially removes the AC component and the DC output forms the

input to the temperature lineariser and controller/programmer described earlier. It is thus possible to carry out high resolution AC resistivity studies either in the isobaric or isothermal mode of measurement. In this set up it is possible to detect changes in resistivity 1 part in 1000.

6. PRESSURE INDUCED SECOND-ORDER TRANSITION IN NICKEL

6.1 Introduction

There has been considerable controversy regarding the existence of a pressure induced second order transition in Nickel, first discovered by Bridgman.[19,20] Bridgman made a number of investigations on a single crystal of Ni, which was pressure seasoned up to 30 kbar. He observed a break in slope in the linear compressibility near 10 kbar and he interpreted this observation as indicative of a pressure induced second order transition. The break in slope near 10 kbar amounts to a discontinuity in the compressibility $\approx 6.9 \times 10^{-8}$ per kg/cm^2 in the direction of an increased compressibility at higher pressure. He also noted that the parameters of this transition changed with successive applications of pressure, the pressure at which discontinuity occurred fluctuating between 10 and 20 kbar and the amount of discontinuity also fluctuating. High pressure resistivity work[19] also indicated an anomalous behavior near 10 kbar. However other studies on compressibility using dilatometric method on both single crystal and polycrystalline sample[21,22] and saturation magnetic moment[23] did not reveal any anomalies in this pressure region.

High resolution TEP and resistivity measurements on well annealed samples of polycrystalline Ni carried out under isothermal conditions with temperature stability $\approx \pm 0.02^{\circ}$C have revealed new features of this phase transition. The second order phase boundary has also been delineated in the P-T plane. We also propose that the anomalies in several of the physical properties near 10 kbar are related to polarity fluctuations between the almost degenerate $3d^8\ 4s^2$ and $3d^9\ 4s^1$ configurations of the Ni pseudo atom in the lattice[24].

6.2 Experimental details

Samples used in the present investigation are high purity Nickel (99.995%) in the form of thin wire of diameter 0.004" for resistivity studies and a rod of diameter 0.04" for thermopower studies. The specimens were annealed in vacuum at 1000°C for six hours, cooled with the furnace and subsequently pressure seasoned to 30 kbar. High pressure experiments were carried out in a conventional piston-cylinder apparatus with a liquid pressure transmitting medium. Silicone oil of viscosity grades 5cst and 150 cst and n-pentane were used in these studies to confirm that the anomalies observed are material properties and not associated with the changes in the visco-elastic properties of the pressure transmitter.

6.3 Results

Figure 5 presents the typical resistance versus pressure data of an isothermal run at 30°C with silicone fluid (viscosity grade 5cst) as the pressure transmitter. The new feature that has emerged out of the present study is the anomalous behavior of resistivity near 12 kbar. The change of sign in the pressure coefficient of resistivity in the 12-14 kbar region clearly points to a subtle phase transition induced by pressure. It must be mentioned that the magnitude of the resistivity peak which is superposed over a curve with negative slope

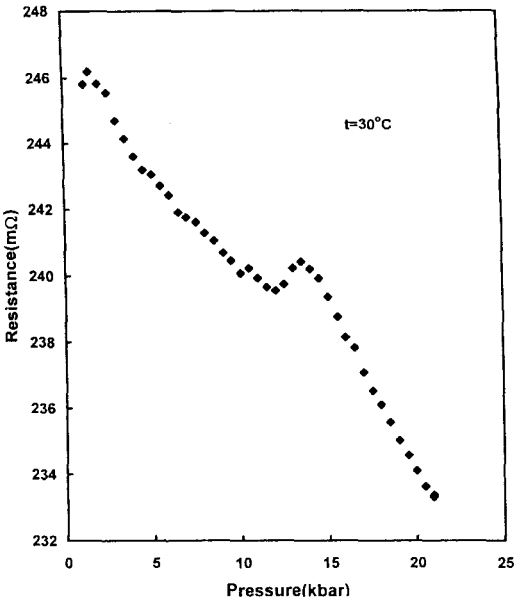

Fig. 5. Resistivity anomaly near 12 kbar

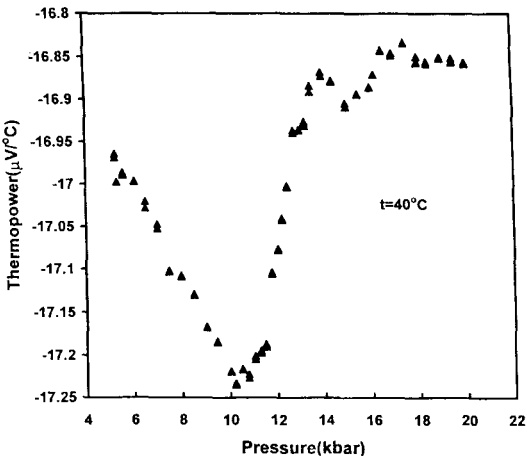

Fig. 6. TEP anomaly near the second order transition

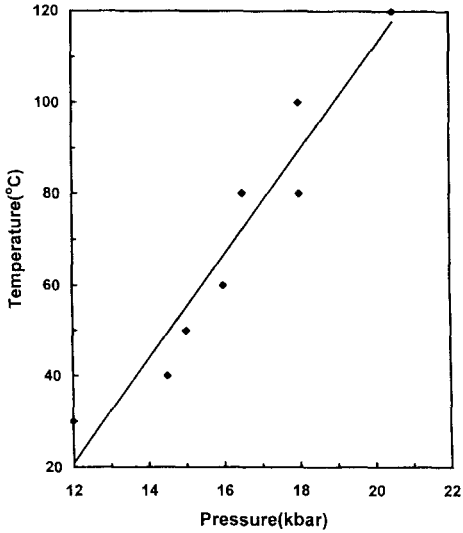

Fig. 7. P-T Phase diagram delineating the second order phase boundary

is small ≈ 0.4% . The non- observation of the resistivity peak in earlier investigations is most probably due to lack of temperature stability of the sample during pressurization. We have observed that it is not possible to observe this feature if the temperature stability of the sample is around 0.5°C. The large temperature coefficient of the resistivity of Nickel swamps the true pressure effect. Extensive studies in our laboratory employing different pressure transmitting media like silicone fluid of viscosity grade 150cst and n-pentane have clearly established that the anomalies observed are intrinsic and not related to any artifacts connected with the change in the viscoelastic properties of the pressure transmitting medium. The pressure coefficient of resistivity deduced here is close to that obtained by Bridgman although the nature of the anomaly is quite different. Higher temperature isotherms show that the resistivity peak broadens out and its position shifts to higher pressures. Further confirmatory evidence for the second order transition is provided by the present measurements of TEP in the same pressure region. Figure 6 is a typical TEP versus pressure plot at 40°C. The nature of the anomaly is quite distinct and occurs in the same pressure region where resistivity behavior is anomalous (Figure 5). Like the resistivity peak, the magnitude of the TEP anomaly is also small ≈± 0.4μV /°C. The magnitude of the TEP anomaly decreases with the increase in temperature and its position shifts to higher pressures similar to that observed in resistivity studies. The resistivity and TEP data have been combined to delineate this phase boundary in the P-T plane and the results are presented in Figure 7.

6.4 Discussion

The present high-resolution TEP and resistivity data clearly establish the existence of a pressure induced continuous phase transformation in nickel. We believe that the pioneering experiments of Bridgman on the compressibility behavior are essentially correct and suggest that the isothermal compressibility is anomalous near 10-12 kbar region. However the nature of this phase transition remains elusive and further experimental work using other microscopic tools is needed to identify the order parameter characterizing this transition. In what follows we present a simple model to explain the anomalies observed in the electronic transport properties of nickel. It is well recognized in the literature that a correct description of the state of electrons in the iron group of transition metals lies between two extremes viz., localized and itinerant models[25] . The itinerant picture derives its strength from data such as d-band specific heats, non-integral magneton numbers and evidence for participation of d-electrons in conduction process. Arguments that favor the localized picture are based on the critical scattering of neutrons, low entropy change across the ferromagnetic transition and the behavior of ferromagnetic moments in alloys. There is now overwhelming evidence from galvanomagnetic data that the d-like electrons are quite mobile and cannot be distinguished from the highly mobile s-type of electrons. Hurwitz[26] and Van-vleck[27] proposed what is known as the minimum polarity model to explain the ferromagnetic and other properties of Ni and related systems. Here the d-electrons are envisioned as distributed among atoms in states closely resembling d^{10} and d^9 states of the free atom, the relative numbers being chosen to fit the data on d-cores. The holes (d^9 configuration) is envisaged as free and can migrate through the lattice with the only requirement that it has to avoid one another. Van-Vleck[27] explained the ferromagnetism of Ni as arising from the participation of d^8,d^9 and d^{10} configurations which exist within an energy range of 1.5 eV. An attractive feature of this model is that it combines both the localized and itinerant aspects of the d-electrons. We believe that this model can also explain the anomalies in the electronic transport properties near the pressure induced second order phase boundary.

7. PRESSURE STUDIES ON THE MAGNETIC TRANSITIONS IN CHROMIUM BASED ALLOYS

7.1 Introduction

Chromium alloy systems exhibit a rich variety of magnetic transitions and have been studied extensively at ambient pressure and also at high pressures[28]. It is well established that these magnetic transitions are associated with the nesting of the Fermi surface. Pure chromium is an itinerant antiferromagnet described as an incommensurate spin density wave below the Neel temperature (311K). This unique type of antiferromagnetic ordering was explained by Lomer[12] and Overhauser[29] as arising due to the attractive coulomb interaction between electron and hole pockets near the Fermi surface which have approximately the same octahedral shape and size. This interaction leads to an energy gap right at the Fermi surface and gives rise to well defined anomalies in electrical resistivity and TEP[30]. Alloying studies have established that there is a correlation between the electron to atom ratio (e/a) and the Neel temperature (T_N) and also the type of antiferromagnetic ordering. For alloying with elements whose e/a < 6, it has been experimentally observed that the magnitude of T_N is lowered and the spin density wave remains incommensurate with the lattice. On the other hand, alloying with

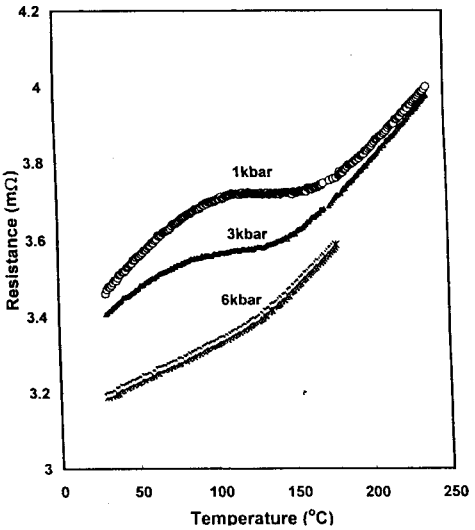

Fig. 8. Resistance vs temperature behavior in $Cr_{0.995}Rh_{0.005}$

elements whose e/a > 6 leads to a rapid increase in T_N and importantly the nature of the spin density wave changes to a commensurate type at a critical concentration. The current experimental and theoretical status in chromium alloys has been excellently reviewed in a recent article by Fawcett et al[28].

The effect of pressure on different magnetic transitions like the commensurate - paramagnetic(C-P), incommensurate - paramagnetic (I-P), and incommenensurate -commensurate(I-C) phases in chromium based alloys are of fundamental interest. The magnetic phase diagram in the pressure temperature plane is remarkably similar to that in the composition - temperature plane in these systems. This observation has led to the general view that increasing pressure is equivalent to alloying chromium with an element whose e/a < 6. Conventionally electrical resistivity, neutron scattering and thermal expansion have been used as tools to track the different magnetic transitions at high pressures[28].

Extensive work has been carried out in our laboratory on several alloy systems like $Cr_{0.99}Rh_{0.01}$, $Cr_{0.995}Rh_{0.005}$, $Cr_{0.95}Mn_{0.05}$, $Cr_{0.99}Re_{0.01}$ and $Cr_{0.995}Re_{0.005}$ where both electrical resistivity and TEP are employed as diagnostic tools to delineate C-P, I-P and C-I magnetic phase boundaries[15-17].

A significant aspect of these experimental studies is that TEP is a convenient tool to track the magnetic phase boundaries especially in the high pressure region where the characteristic resistivity anomaly vanishes. Further the temperature behavior of TEP is markedly different in the commensurate and incommensurate phases which can be used as a signature for the phase transition. In what follows we review the data on two alloy systems viz., $Cr_{0.995}Rh_{0.005}$ and $Cr_{0.95}Mn_{0.05}$.

7.2 Magnetic transitions in $Cr_{0.995}Rh_{0.005}$

In Cr-Rh system it is well established[31] that at a critical concentration around 0.11 atomic% of Rh the spin density wave (SDW) becomes commensurate with a marked increase in the magnitude of T_N. Thus the alloy under study viz., $Cr_{0.995}Rh_{0.005}$ is characterized by a commensurate SDW at ambient pressure and temperature conditions. Figure 8 gives the plot of resistance versus temperature at different pressures up to 6 kbar. The resistivity anomaly near T_N manifests as a weak minimum for this alloy system. The anomaly near 175°C at 1 kbar is thus associated with the commensurate-paramagnetic (C-P) phase transition. Pressure has a marked effect on the nature of the resistivity anomaly accompanied by a strong depression in the magnitude of T_N. It may be noted that at a pressure of 6 kbar, the C-P transition manifests as a change of slope near 120°C. The data corresponding to higher pressure isobars are presented in Figure 9. We note that the characteristic resistivity anomaly almost vanishes in the region beyond 12 kbar and it is impossible to track this phase boundary at higher pressures.

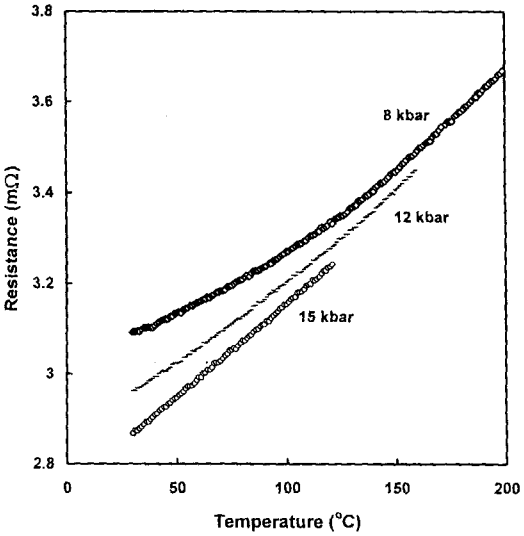

Fig. 9. Higher pressure isobars of resistance vs temperature

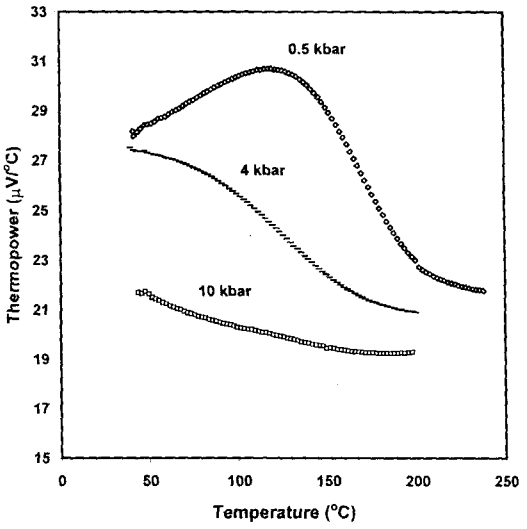

Fig. 10. TEP vs temperature in the low pressure region

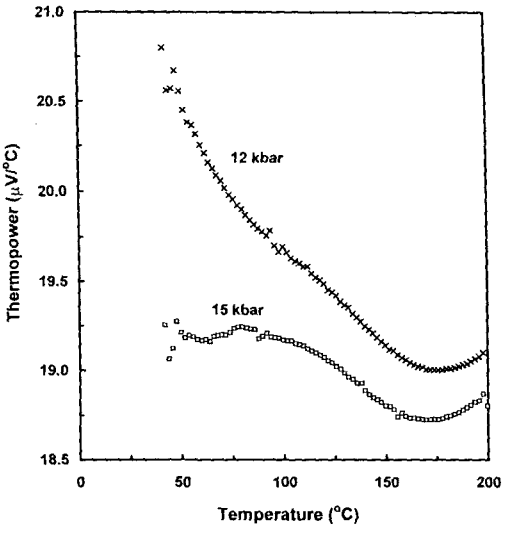

Fig. 11. Crossover from C-P to I-P at higher pressures

Figure 10 gives the data of absolute TEP versus temperature for several isobars up to 10 kbar. As viewed from the high temperature side, TEP exhibits a marked increase in its magnitude as the sample is cooled below T_N. For the 0.5 kbar isobar, T_N is around 200°C and the magnitude of the TEP anomaly is around 9 μV/°C. This large TEP anomaly is in sharp contrast to the rather weak resistivity anomaly shown in Figure 8. We also note that the position of the peak in the TEP versus temperature plot shifts to lower temperatures with increase in pressure. The pressure coefficient of T_N associated with C-P transition is rather large ≈ -5°C/ kbar and can be easily estimated using TEP anomaly as a marker. Figure 11 gives the behavior of TEP for two isobars at 12 and 15 kbar. The 12 kbar isobar is clearly associated with the C-P transition. There is a distinct change in the nature of the TEP anomaly at higher pressures as reflected in the data corresponding to 15 kbar isobar. Firstly the position of the peak in the TEP versus temperature plot has shifted to higher temperatures (≈80°C) whereas one would have expected this peak to occur at a temperature lower than 40°C had the commensurate phase been stable in this pressure region. Secondly the magnitude of the TEP anomaly has reduced considerably at this isobar. This data clearly indicates that at a critical pressure between 12 and 15 kbar, the commensurate SDW (C- Phase) changes over to an incommensurate SDW (I-phase). The Neel temperature for the 15 kbar isobar is associated with the I-P transition. Figure 12 presents the TEP data on an expanded scale corresponding to 20 and 23kbar pressure. The scatter in the data is ± 0.01μV/°C. It is worth noting that the characteristic anomaly near T_N is still observable. In this pressure region the shift of T_N with pressure

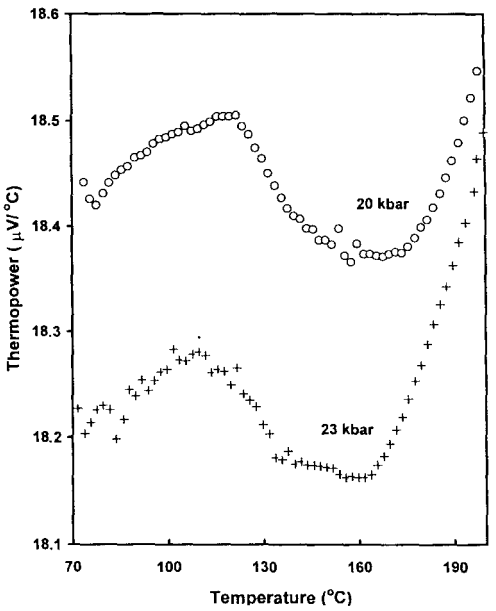

Fig. 12. High resolution TEP data across I-P transition

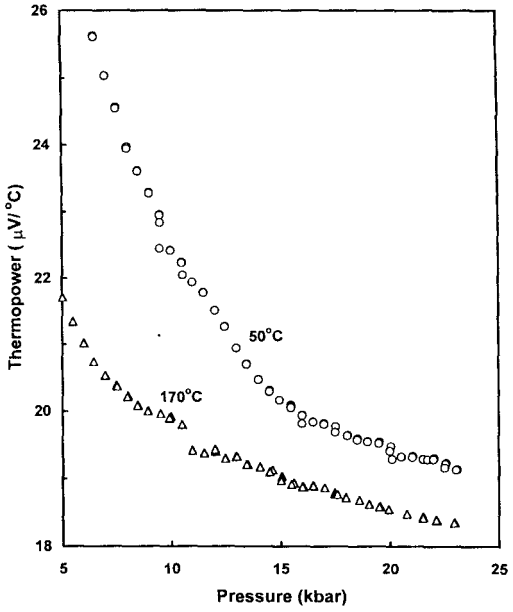

Fig. 13. TEP anomaly near C-I phase boundary

is small ≈ -2°C/kbar which is typical for the slope of the I-P phase boundary. The present experimental studies clearly indicate that TEP is a powerful diagnostic tool to track the magnetic phase boundaries especially in the higher-pressure regime. Moreover TEP exhibits clear signatures marking a crossover from the C-P to I-P transition.

The commensurate to incommensurate (C-I) phase transition is subtle in the sense that both these phases have nearly the same energy and is continuous except in systems like CrMn and CrFe. Resistivity does not exhibit any anomaly across this transition. We have tried to locate this phase boundary in the P-T plane through careful measurements of TEP. Figure 13 presents TEP data as a function of pressure for two isothermal runs at 50°C and 170°C. In these experiments the mean temperature of the sample was held constant to within ± 0.02°C during pressurization. We observe distinct anomalies near 9.5 kbar for the 50°C isotherm and near 10.75 kbar for the 170°C. These anomalies are associated with the C-I phase transition. The slope of the C-I phase boundary is positive and large ≈ 100°C/kbar. The magnetic phase diagram for this alloy system delineating C-P, I-P and C-I phase boundaries in the P-T plane is given in Figure 14. The coexistence of the three distinct magnetic phases (C,I,P) at a point with coordinates 10.5 kbar and 170°C signifies the occurrence of a triple point.

7.3 Magnetic transitions in $Cr_{0.95}Mn_{0.05}$

The critical concentration for the Cr-Mn alloy system where the magnetic structure changes over from the incommensurate to the commensurate type is around 0.3 atomic % Mn. Thus the alloy under study is already in the commensurate phase characterized by a high T_N of 320°C at ambient pressure. The C-P transition as studied through resistivity at 3 kbar is shown in Figure 15. The resistivity minimum occurs near 240°C corresponding to the Neel temperature showing that pressure has a large effect in the commensurate phase. Higher pressure isobars where resistivity anomaly is used to track the C-P phase boundary are given in Figure 16. The resistivity anomaly vanishes in the pressure region beyond 15 kbar indicating that resistivity tool is ineffective in delineating magnetic phase

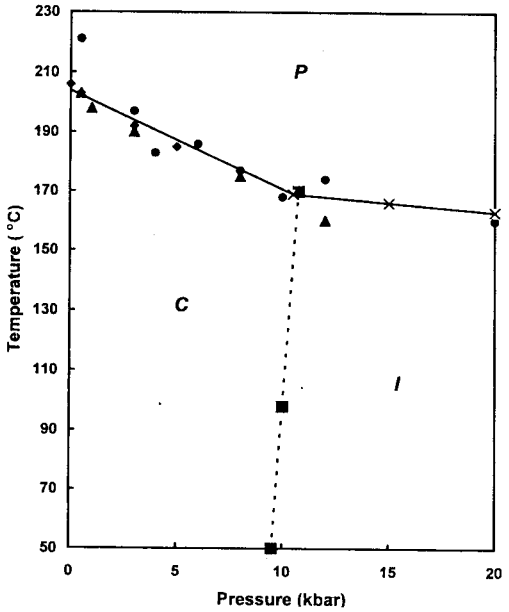

Fig. 14. Magnetic phase diagram of $Cr_{0.995}Rh_{0.005}$

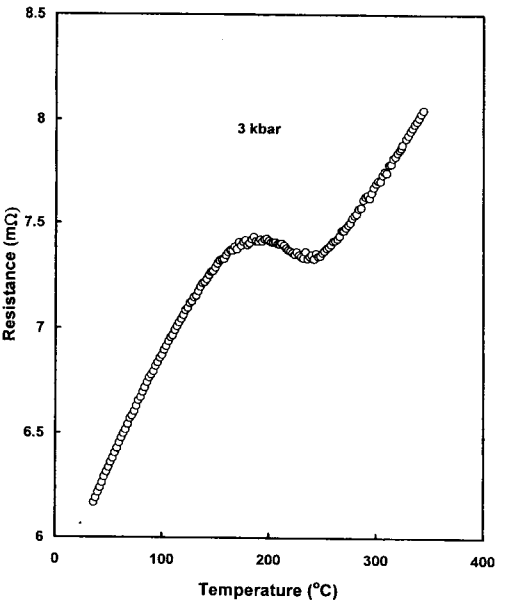

Fig. 15. Resistivity anomaly near C-P transition in $Cr_{0.95}Mn_{0.05}$

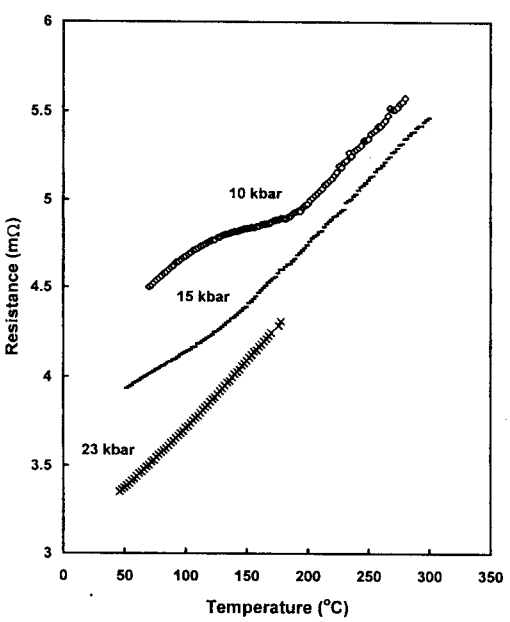

Fig. 16. Resistivity anomaly across C-P transition at higher pressures

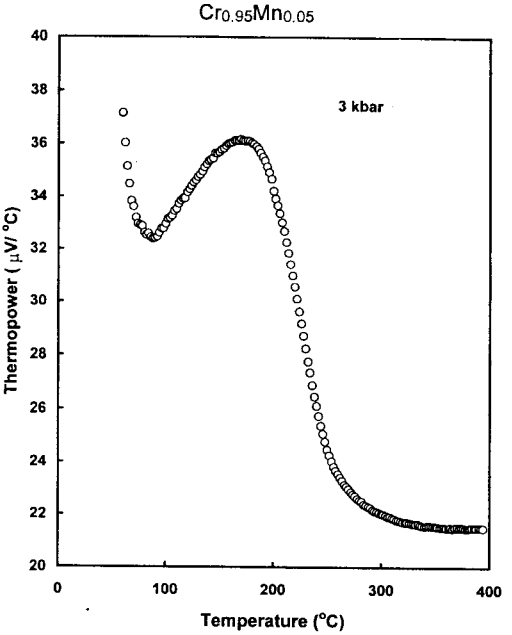

Fig. 17. TEP anomaly across C-P transition

boundaries at higher pressures. Results of the TEP studies across the C-P transition are given in Figure 17. The C-phase has a large value of TEP of $\approx 35\mu V/^{o}C$ and the C-P phase transition manifests as a sharp decrease in the magnitude of TEP. The P-phase has a smaller value of TEP $\approx 21\mu V/^{o}C$. As viewed from the high temperature side, TEP exhibits marked increase in its magnitude as the sample is cooled below T_N and reaching a maximum at a temperature lower than T_N. The TEP anomaly $\approx 14\mu V/^{o}C$ across the C-P transition should be contrasted with the rather weak resistivity anomaly observed at the same pressure (Figure 16). It is this feature which makes TEP technique a versatile tool to

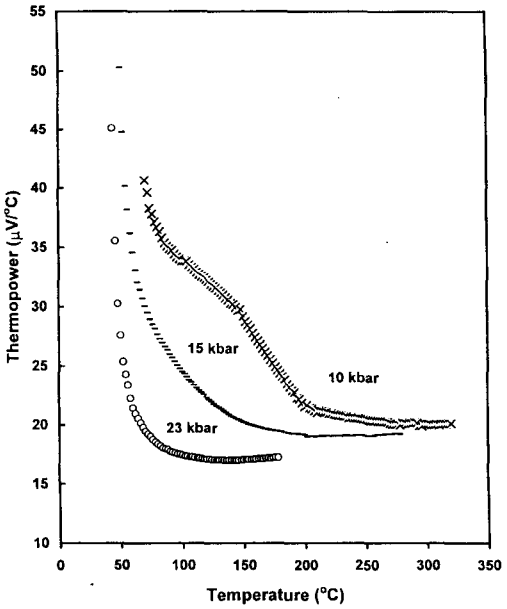

Fig. 18. Higher pressure isobars of TEP vs temperature

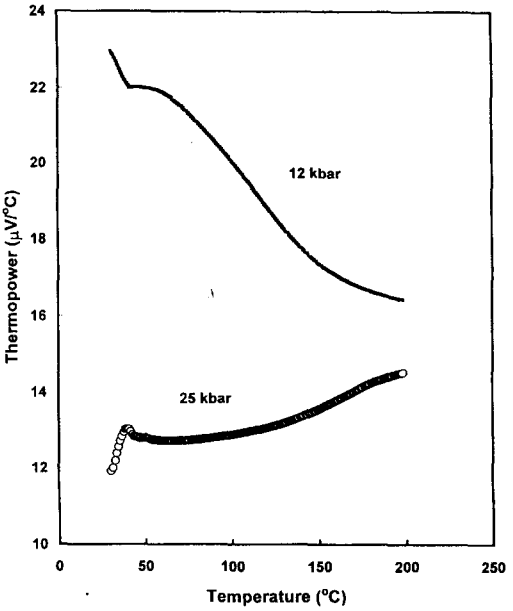

Fig. 19. Cross-over from C-P to I-P transition

probe the magnetic phase boundaries in the pressure regime where the resistivity behavior is devoid of observable anomalies. Figure 18 gives several isobars of TEP versus temperature. It is important to note that in contrast to the resistivity behavior, TEP exhibits distinctive anomalies even at pressures higher than 15 kbar. The temperature behavior of TEP at two different isobars viz., 12 and 25 kbar is shown in Figure 19. The magnitude of TEP corresponding to 12 kbar isobar is higher and has a negative temperature coefficient. At pressures beyond 25 kbar, the magnitude of TEP is small and the temperature coefficient is positive. We believe these features signal the crossover from C-P transition at 12 kbar to I-P transition at 25 kbar.

7.4 Discussion

The anomalies in the electronic transport properties in chromium based alloys are related to its peculiar energy band structure. It is well known that the attractive Coulomb interaction between electrons and holes in two different sheets of Fermi surface separated by a wave vector Q in the (100) direction leads to an energy gap in the single particle spectrum. Essentially a part of the Fermi surface is wiped out at the Neel temperature due to this attractive interaction and leads to well defined anomalies in the electronic transport properties. The present experimental results, especially those on TEP can be qualitatively understood on the basis of a model developed by Trego and Mackintosh[11]. Although the arguments presented in this model are applicable to the incommensurate phase, qualitatively the same results hold good for the commensurate phase as well. The diffusion part of TEP is related to the energy derivative of the density of states and the carrier relaxation time evaluated at the Fermi energy. Although the density of states undergoes a marked decrease at the antiferromagnetic phase transition due to the opening up of an energy gap, the energy derivative of the density of states is not expected in this model to undergo drastic changes. Thus the major contribution to TEP stems from the energy derivative of the electron-phonon relaxation time evaluated at the Fermi energy. The electron-phonon scattering that determines the relaxation time is drastically affected due to the energy gap 2Δ right at the Fermi energy. Since the number of final

states into which an electron at the Fermi surface can be scattered by a phonon is highly reduced, this has the effect of increasing the relaxation time. Modeling the phonon spectrum as Debye type, these authors evaluated the energy derivative of the relaxation time for various values of Δ. It turns out that this term makes a positive contribution to TEP and assuming that this is the dominant effect one can account for its positive sign. It should also be noted that the energy gap 2Δ in the antiferromagnetic phase is temperature dependent becoming zero at T_N. Thus as the gap increases from a value smaller than the characteristic energy of the phonon to a value higher than this energy, TEP exhibits a positive maximum at a temperature below T_N. Experimentally this type of variation is observed in pure chromium and its alloys. The present high pressure data further corroborate the implications of this model. We note here that the energy gap parameter $2\Delta(T)$ is pressure dependent, decreasing with pressure at different rates in the commensurate and incommensurate phases. The magnitude of the hump in the TEP versus temperature plot (Figure 17), characteristic of the commensurate phase with $\Delta \approx$ 0.4eV, decreases with increase in pressure and the peak position shifts to lower temperatures. This is in agreement with the predictions of this model where the peak in the TEP versus temperature plot is identified with the condition $\Delta(P) \approx$ energy of the phonon. This criterion can also be used to identify the crossover from the C-P to I-P magnetic transition. The hump in the TEP plot is expected to be smaller across the I-P transition in view of the fact that the I-phase has a much smaller value for Δ which is typically around 0.1eV. The experimental findings in Figure 19 thus provide direct evidence for the crossover from the commensurate to the incommensurate phase.

ACKNOWLEDGEMENTS

It is a pleasure to thank Dr A K Singh for his keen interest in the work reported in this paper. We thank the present and the past Directors for their support to the High pressure research activity at NAL. We would also like to thank Dr A Jayaraman for providing us with the samples of Chromium alloys and Mr K J Rao for skilful mounting of the high pressure cells.

REFERENCES

1. Barnard, R. D. in: Thermoelectricity in Metals and Alloys, Taylor & Francis, London, 1972.
2. Bridgman, P. W, in: The Physics of High Pressure, G. Bell Sons, London, 1958, p.295.
3. Reshamwala, A. S. and Ramesh, T. G., J. Phys. E, 1974, **7,** 133.
4. Reshamwala, A. S. and Ramesh, T. G., J. Phys. E, 1975, **8,** 465.
5. Shubha, V. and Ramesh, T. G., J. Phys. E, 1976, **9,** 435.
6. Shubha, V. and Ramesh, T. G., High Temp. High Pressure, 1986, **18**, 311.
7. Shubha, V. and Ramesh, T. G., Rev. Sci. Instrum., 1986, **57**, 473.
8. Shubha, V. and Ramesh, T. G., in: Advances in Instrumentation, Eds., B. S. Ramprasad et al, New Age International (P) Ltd, Bangalore, 1996, pp. 98-103.
9. Shubha, V. and Ramesh, T. G., High Temp. High Pressure, 1977, **9**, 461.

10. Shubha, V. and Ramesh, T. G., in: Recent Trends in High Pressure Research, Ed., A.K.Singh, Oxford & IBH Co. Pvt. Ltd., New Delhi, 1992, pp. 283-85.
11. Trego, A.L. and Mackintosh, A.R., Phys. Rev., 1968, **166**, 495.
12. Lomer, W. M., Proc. Phys. Soc. London, 1962, **80**, 489.
13. Jayaraman, A., Rice, T. M. and Bucher, E., J. Appl. Phys., 1970, **41,** 1970.
14. Syono, Y. and Ishikawa, Y., Phys. Rev. Lett., 1967, **19**, 747.
15. Ramesh, T. G and Shubha, V., in: Recent Trends in High Pressure Research, Ed., A.K.Singh, Oxford & IBH Co. PVT. LTD, New Delhi, 1992, pp. 53-55.
16. Ramesh, T. G. and Shubha, V., in: Advances in High Pressure Science & Technology, Ed., A. K. Singh, Tata McGrawHill, New Delhi, 1995, pp. 75-83.
17. Shubha, V. and Ramesh, T. G., in: Advances in High Pressure Science & Technology, Eds., M.Yousuf et al, Universities Press (India) LTD, 1997, pp. 178-81.
18. Jayaraman, A., Hudson, R., McFee, J. H., Coriell, A. S. and Maines, R. G., Rev. Sci. Instrum., 1967, **38**, 44.
19. Bridgman, P. W., Proc. Am. Acad. Arts. Sci., 1949, **77,** 189.
20. Bridgman, P. W., Proc. Am. Acad. Arts. Sci., 1951, **79,** 149.
21. Kutsar, A. R., Fiz. Met. Metalloved., 1971, **32**, 886.
22. Vaidya, S. N. and Kennedy, G. C., J. Phys. Chem. Solids, 1970, **30**, 2329.
23. Jatsumoto, E., Fujwara, H., Tange, J. and Hiraoka,T., J. Phys. Soc. Jpn., 1963, **18**, 1348.
24. Ramesh, T. G. and Shubha, V., in: Advances in High Pressure Science & Technology, Ed., A. K. Singh, Tata McGrawHill, New Delhi, 1995, pp. 65-74 and references therein.
25. Herring, C., in: **Magnetism,Vol. IV**, Academic Press, NY, 1966, pp 118-145.
26. Hurwitz, H., Thesis, Harvard Univ., Cambridge, Massachusetts, 1941.
27. Van-Vleck, J. H., Rev. Mod. Phys., 1953, **25**, 220.
28. Fawcett, E., Alberts, H. L., Galkin, V.Yu., Noakes, D. R. and Yakhmi, J. V., Rev. Mod. Phys., 1994, **66,** 25 and references therein.
29. Overhauser, A. W., Phys. Rev., 1962, **128,** 1437.
30. Arrott, A., in: Magnetism, Eds., G. Rado and H. Suhl, Academic, NY, 1966, **IIB,** 295.
31. Butylenko, A. K. and Nevdacha, V. V., Dokl. Akad. Nauk. Ukr. Ssr. ser.A, 1980, **5,** 67.